ACS NANO

Cite This: ACS Nano XXXX, XXX, XXX–XXX

www.acsnano.org

ARTICLE

Manipulation and Deposition of Complex, Functional Block Copolymer Nanostructures Using Optical Tweezers

Oliver E. C. Gould,[†,#] Stuart J. Box,[‡] Charlotte E. Boott,[†] Andrew D. Ward,[§] Mitchell A. Winnik,[∥] Mervyn J. Miles,[*,‡] and Ian Manners[*,†,⊥]

[†]School of Chemistry, University of Bristol, Bristol BS8 1TS, United Kingdom

[‡]School of Physics, University of Bristol, Bristol BS8 1TL, United Kingdom

[§]Central Laser Facility, Rutherford Appleton Laboratories, Oxford OX11 0QX, United Kingdom

[∥]Department of Chemistry, University of Toronto, Toronto, Ontario M5S 3H6, Canada

[⊥]Department of Chemistry, University of Victoria, Victoria, British Columbia V8W 3V6, Canada

Supporting Information

ABSTRACT: **Block copolymer self-assembly has enabled the creation of a range of solution-phase nanostructures with applications from optoelectronics and biomedicine to catalysis. However, to incorporate such materials into devices a method that facilitates their precise manipulation and deposition is desirable. Herein we describe how optical tweezers can be used to trap, manipulate, and pattern individual cylindrical micelles and larger hybrid micellar materials. Through the combination of TIRF imaging and optical trapping we can precisely control the three-dimensional motion of individual cylindrical block copolymer micelles in solution, enabling the creation of customizable arrays. We also demonstrate that dynamic holographic assembly enables the creation of ordered customizable arrays of complex hybrid block copolymer structures. By creating a program which automatically identifies, traps, and then deposits multiple assemblies simultaneously we have been able to dramatically speed up this normally slow process, enabling the fabrication of arrays of hybrid structures containing hundreds of assemblies in minutes rather than hours.**

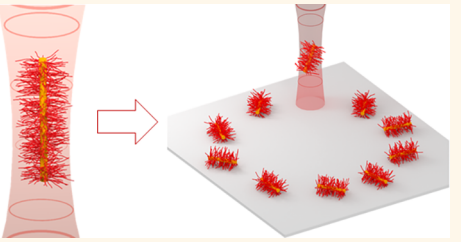

KEYWORDS: *optical trapping, block copolymers, self-assembly, directed assembly, nanofibers*

Nature is adept at controlling the organization of complex multicomponent systems over length scales from nanometers to micrometers. For synthetic materials the use of bottom-up approaches, such as self-assembly, has enabled the creation of nanoscale assemblies from a diverse range of molecular and polymeric species. However, because of the inherently stochastic nature of self-assembly, which is reliant on controlling the random interactions of nanoscale subunits, this approach has often struggled to navigate the kinetic traps which plague hierarchical assembly across multiple length scales. Additional methods are therefore needed that marry top-down and bottom-up approaches to yield greater deterministic control over material design and to produce functional materials across multiple hierarchical levels. Such approaches aim to control the thermodynamic landscape that governs the organization of the nanoscale components, potentially enabling their incorporation into devices and realizing emergent macroscale behavior.

The solution-phase self-assembly of block copolymers has emerged as a promising bottom-up method to produce a broad range of nanoscale soft-matter structures with potential applications in optoelectronics, biomedicine, and catalysis in addition to other fields.[1−10] Spheres, cylinders, platelets, and more complex morphologies have all been produced through variations of the block ratio, overall molar mass, and experimental conditions such as temperature, solvent, and concentration.[5−7] The functionalization of these nanoparticulate materials has been achieved either through manipulation of the component polymer chemistries or by the use of templating approaches.[8−11] However, despite their promise, the use of block copolymer micelles in a variety of applications has been limited by difficulties in controlling the transfer of such structures into the solid state. In particular, methods are needed that enable the fast and efficient manipulation of micelle-based materials and allow control over the density and placement of individual elements in large-scale arrays.

Received: January 15, 2019
Accepted: February 22, 2019
Published: February 22, 2019

DOI: 10.1021/acsnano.9b00342
ACS Nano XXXX, XXX, XXX–XXX

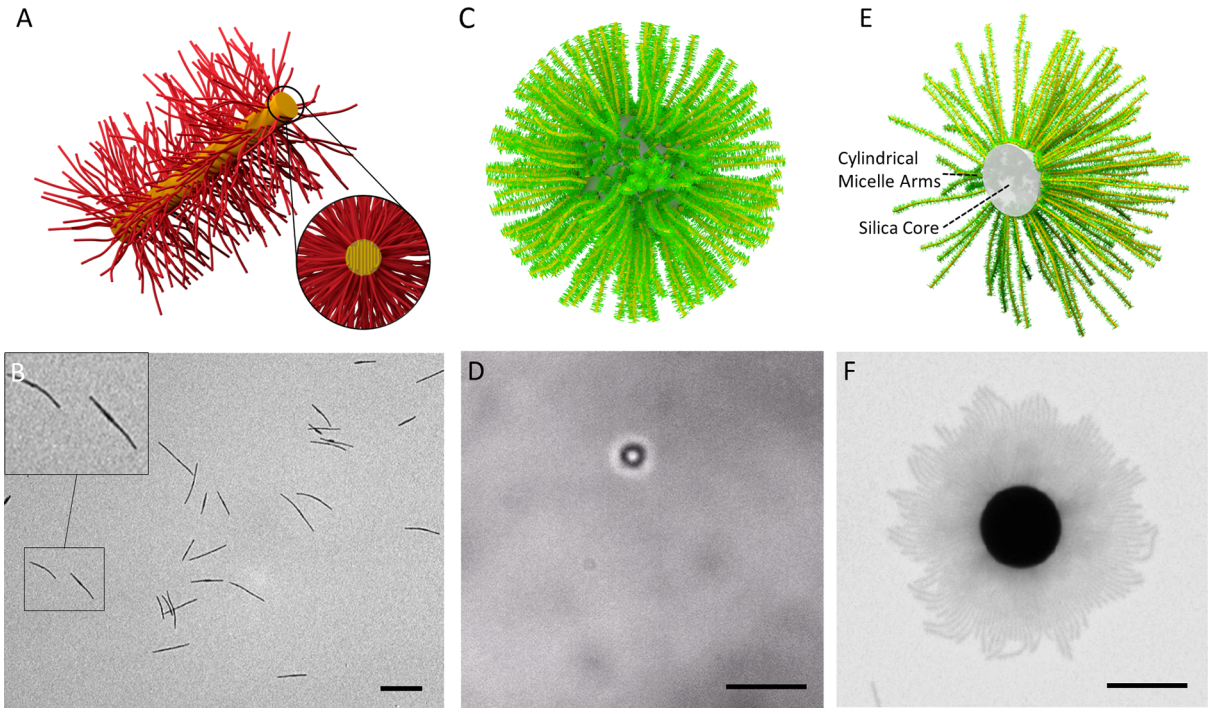

Figure 1. (A) Graphical representation of a PFS-b-PDMS cylindrical micelle with a bodipy dye-functionalized corona. (B) TEM image showing the cylindrical micelles drop cast from solution. Scale bar is 1 μm. (C, E) Schematic showing hybrid dandelion structure and cross section. Images of hybrid dandelion structure taken by (D) brightfield optical microscopy and (F) TEM. Scale bars are 5 and 1 μm, respectively.

A number of methods for the formation of ordered arrays from solution-phase dispersions of 1D-nanomaterials have been demonstrated. For metallic nanowires these can be separated into those that utilize external fields, such as dielectrophoresis[12,13] or magnetic field-based approaches,[14] and those that use shear, such as Langmuir−Blodgett,[15,16] fluid-flow directed,[17−19] and nanocombing[20,21] processes. Despite the development of such a diverse range of techniques, few have been successfully applied to block copolymer micelles, which exhibit limited interaction with external fields and are generally relatively fragile unless core- or corona cross-linking is performed.

Since their introduction in 1970,[22] optical tweezers have become an important tool for the manipulation of colloidal materials. By harnessing the interaction of light with dielectric objects such techniques have allowed for unmatched control over the movement of a variety of high refractive index, solution-phase materials. Optical manipulation has found widespread applicability to micro/nanofabrication and assembly,[23−25] with particular benefit for fragile objects where noncontact manipulation is highly desirable.[26−28] Important recent work in this area has demonstrated manipulation speeds using optical tweezers of 170 and 150 μm/s for dielectric and metallic nanoparticles, respectively.[29] This work shows optical tweezers' ability to compete with other common, serial rapid prototyping and nanofabrication approaches in both speed and precision.

While the optical trapping of polymer latex particles is now commonplace, for self-assembled micelles based on amphiphilic copolymers this has only been achieved for uncontrolled clusters in the form of micrometer-sized particles[30−32] or, more recently, for large supermicelle assemblies (approximately 5 μm) by our group.[33] Key challenges are to show the controlled manipulation and deposition of individual structures but also provide routes to the scalable production of devices and arrays. Herein, we describe how, through the use of optical tweezer techniques, precise three-dimensional control over individual cylindrical or fiber-like micelles can be achieved, as well as the automated formation of arrays.

RESULTS

Preparation of Individual Cylindrical Micelles. The preparation of cylindrical or fiber-like micelles by the solution self-assembly of a diverse array of block copolymers (BCPs) with crystallizable core-forming blocks has now been reported.[34−47] In particular, stable cylindrical micelles with a polyferrocenylsilane (PFS)[48] core can be produced with controlled length and varied functionality through seeded growth protocols. A wide range of functionalization routes for PFS micelles has been reported, including the incorporation of fluorescent dyes,[8,9] and templating to form metals oxide nanowires[10] making them interesting for a variety of applications. The high refractive index of PFS[49] should make these cylindrical micelles promising candidates for optical manipulation. Unfortunately, research in this area has been limited by the difficulty of visualizing individual micelles in solution as their dimensions are far below the diffraction limit of light. While traditional laser fluorescence techniques have been successful in imaging dye-functionalized block copolymer nanostructures over relatively short time scales,[8] the photobleaching of most commonly available dyes has made the continuous monitoring of micelles for the long time periods required for manipulation difficult. Here we use total internal reflection fluorescence microscopy (TIRF) to overcome this problem, enabling the optical manipulation of individual micelles. TIRF operates by utilizing the evanescent wave generated at the glass−solution interface when the incident beam undergoes total internal reflection. As this wave decays exponentially away from the interface, visualization of a very specific axial slice (around 100 nm) of the solution is possible.

DOI: 10.1021/acsnano.9b00342
ACS Nano XXXX, XXX, XXX−XXX

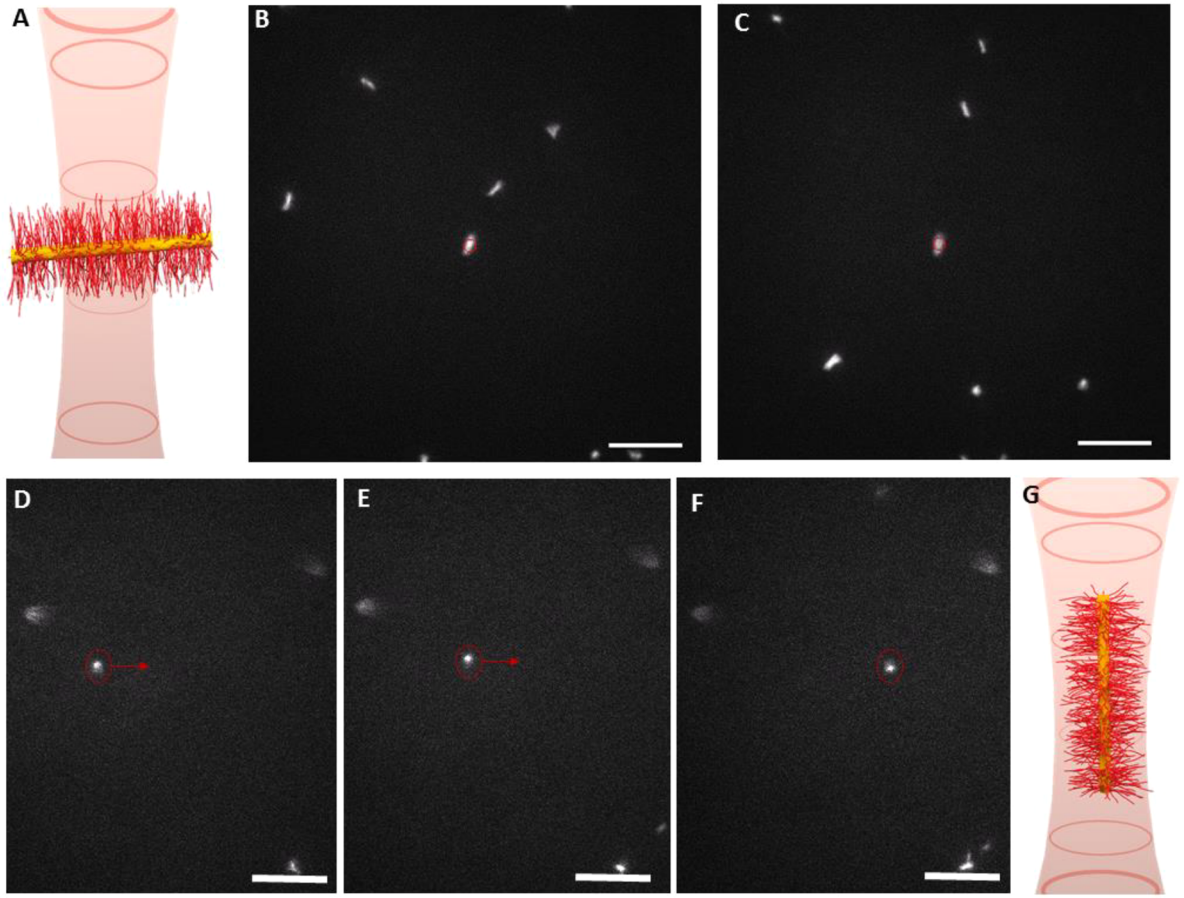

Figure 2. (A, G) Schematic illustrating the optical trapping of a single cylindrical micelle. (B, C) TIRF images of a single micelle (L_n = 1073 nm) trapped perpendicular to the incident beam. (D−F) TIRF images showing the translation of a single cylindrical micelle held in an optical trap. The position of the trapping beam is shown by the red rings, and the direction of movement is indicated by the red arrows. Scale bars are 5 μm.

By imaging such a narrow range of the *z* axis the majority of the background fluorescence from latent cylindrical micelles is removed, enabling visualization at low laser power and thus greatly reducing photobleaching.

To enable the visualization of single cylindrical PFS-*b*-PDMS (PDMS = poly(dimethylsiloxane), block ratio 1:ca. 14) micelles in solution, a 4,4-difluoro-4-bora-3*a*,4*a*-diaza-*s*-indacen (bodipy) dye was grafted onto the polysiloxane corona-forming segment containing a small percentage of vinyl groups via a thiolene "click" reaction as has been reported previously.[8] To prepare the cylindrical micelles, a solution of the block copolymer in THF (a good solvent for both blocks where the polymer exists in the form of unimers) was added to a selective solvent for the corona-forming block (*n*-hexanes). The resulting cylindrical micelles were then sonicated to form crystallite seeds, before additional unimer was added in solution to create uniform monodisperse cylindrical micelles approximately 1000 nm in length (length dispersity = 1.03). The cylindrical micelles consist of an approximately 7 nm diameter crystalline PFS core (estimated by TEM measurements and in accordance with previous work),[50] with a refractive index of ca. 1.6[49] and a solvated PDMS corona (Figure 1A). It is the high-refractive-index PFS core which enables the optical manipulation of the micelles.[33]

A drop-cast transmission electron microscope (TEM) image of the micelles is shown in Figure 1B. The images show only a few aggregated bundles, consistent with the micelles being well dispersed in solution, a characteristic that has been demonstrated by other techniques.[8]

Optical Trapping. A custom-built microscope based around a Nikon Eclipse Ti Chassis fitted with a Nikon Apo TIRF objective ×100 NA 1.49 was used for both TIRF illumination and optical trapping. For the TIRF imaging a 10 μL drop of micelle solution in hexanes was placed on a glass slide before a coverslip was placed on top and sealed. Initial inspection of the samples showed clearly visible, well-dispersed, and highly mobile cylindrical micelles in solution (Supporting Information Figure 1). The low laser power used meant that photobleaching took in excess of 5 min to render the micelles imperceptible.

When a laser trap was created in close proximity to a PFS-*b*-PDMS cylindrical micelle (number-average length L_n = 1073 nm, PDI = 1.03), the micelle was pulled into the trap and held in a stable state in three dimensions. As has been predicted for other crystalline rod-like systems, the cylindrical micelles generally became orientated parallel to the trapping beam (Figure 2D−F). Nevertheless, in certain cases when there was significant flow present, either due to convection currents or because it was created with a syringe pump, the micelles were observed to trap perpendicularly to the trapping beam (Figure 2B,C). Manipulation of the cylindrical micelles in solution was achieved by translating the stage. In this way, complete three-dimensional control over the position of a single micelle was possible (Figure 2D−F and Supporting Information Video 1).

DOI: 10.1021/acsnano.9b00342
ACS Nano XXXX, XXX, XXX−XXX

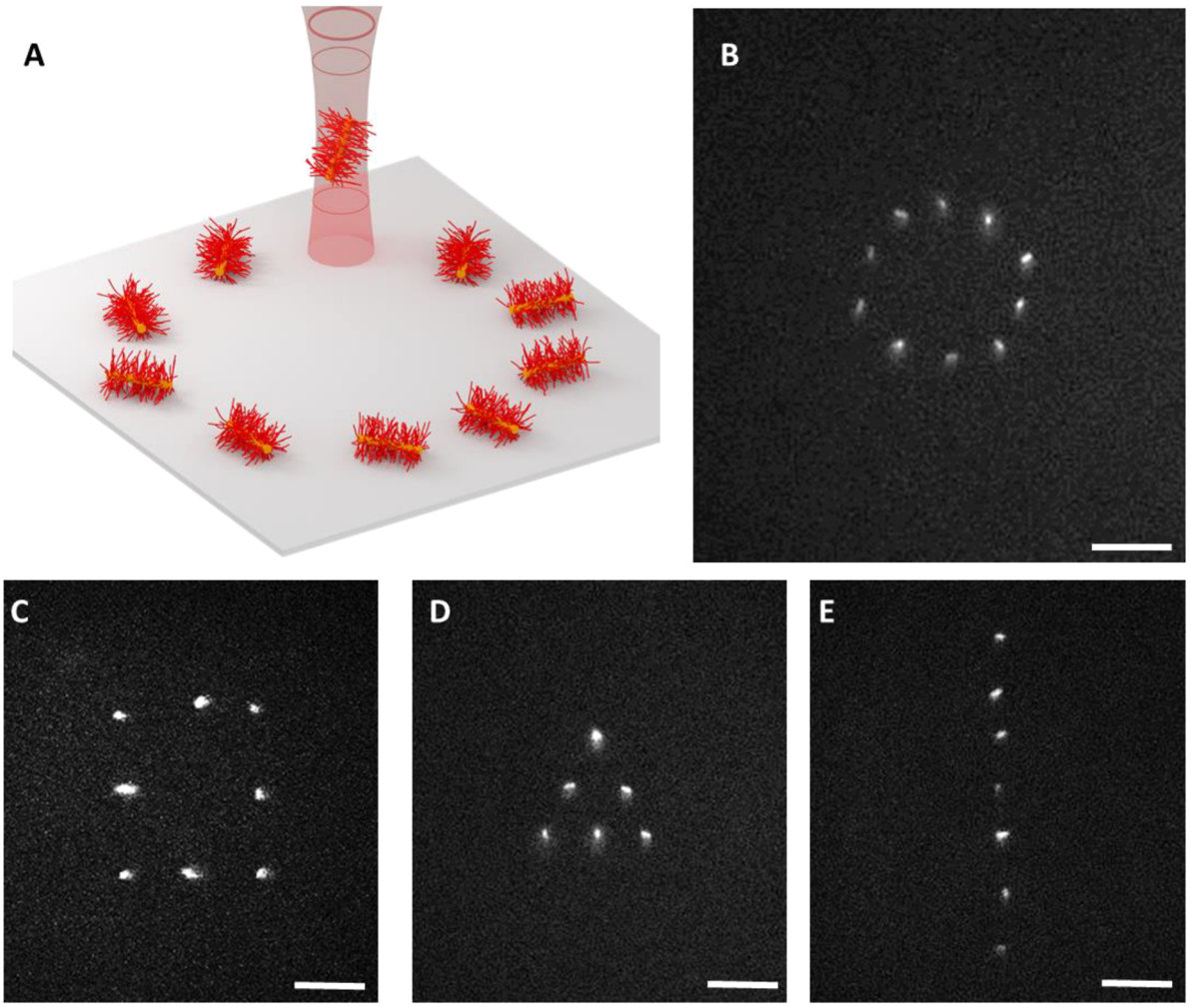

Figure 3. (A) Graphical representation of a circular array of cylindrical micelles. (B–E) TIRF images showing arrays formed by the deposition of trapped cylindrical micelles (L_n = 1073 nm) onto the glass surface using optical tweezers. Scale bars are 5 μm.

Deposition To Form Customized Single Micelle Arrays. Solution-phase block copolymer self-assembly has yielded a range of complex colloidal structures with varied functionality, including luminescent nanopixels,[8,51] theranostic[52] and magnetic[10,53] materials, and electroactive nanowires.[54−56] The development of methods to control the deposition of such soft-matter structures could lead to hierarchical nanostructures with applications in a variety of fields. Using optical manipulation we can direct the deposition and immobilization of individual cylindrical micelles (Figure 3). By trapping individual cylindrical micelles and moving them into the bottom side of the glass channel, the micelles became immobilized and resistant to further movement. Some control over the orientation of the deposited micelle was achieved by placing one end of the trapped cylindrical micelle against the surface and then moving the trap to direct the alignment of the micelle during deposition, as has been demonstrated for metallic nanorods elsewhere.[57] With this method we were able to produce arrays of arbitrary design, including a circle (Figure 3B), a square (Figure 3C), a triangle (Figure 3D) and a line (Figure 3E). The orientation of the micelle was deemed to be the most significant limit on the positional accuracy of the deposition, which was measured as 219 ± 120 nm. The use of smaller micelles and a visualization method with higher resolution would greatly reduce this value.

Deposition of Hybrid Structures. We also demonstrate the automated creation of ordered customizable arrays of block copolymer structures. By using dynamic holographic assembly with an image matching and collision avoidance algorithm, arrays containing hundreds of objects can be fabricated quickly and efficiently. The use of a spatial light modulator (SLM) enables the creation of multiple traps and the manipulation of multiple structures simultaneously.[58] This multiplexing approach significantly improves throughput, but involves sharing the laser beam between multiple traps reducing the time-averaged optical power in each trap. To improve the trapping efficiency, and thereby the reliability and speed of manipulation, we use hybrid micelle-nanoparticle "dandelion" materials recently described elsewhere by Jia et al.[59] These are formed by coating a 900 nm silica bead with short PFS-*b*-P2VP (P2VP = poly-2-vinylpyridine) micelle seeds and which subsequently act as nucleation sites for the growth of long cylindrical micelle arms which enable easy deposition and functionalization. The uniform, isotropic and high refractive index silica core leads to a high trap stiffness and a relatively predictable interaction with light making the optical manipulation of the hybrid structures significantly more efficient.

Visualization and Trapping. Initial experiments confirmed that the dandelion structures were easily visualized using a bright-field optical microscope (Figure 1) and could be

DOI: 10.1021/acsnano.9b00342
ACS Nano XXXX, XXX, XXX−XXX

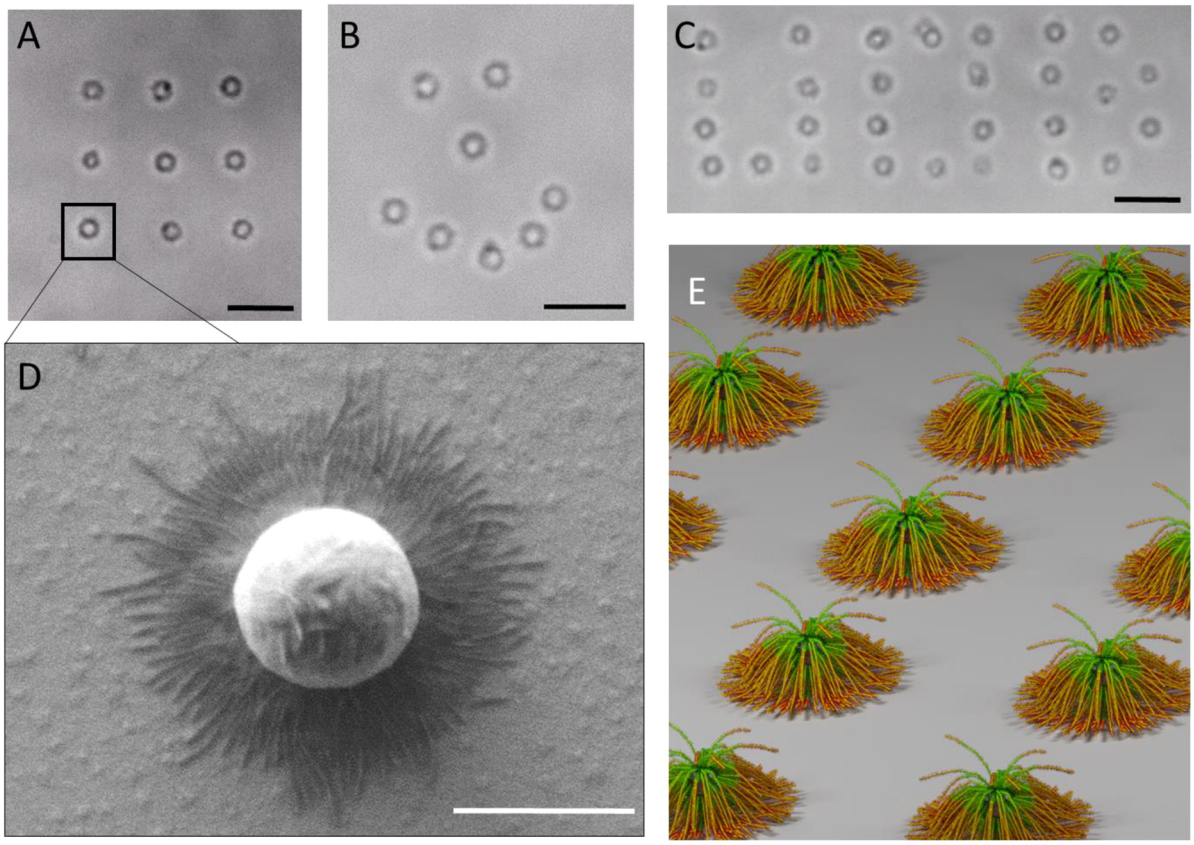

Figure 4. (A–C) Brightfield optical microscope images of customized patterns created by deposition of multiple hybrid dandelion structures in solution. Scale bars are 3 μm. (D) SEM image showing a single deposited hybrid structure. Scale bar is 1 μm. (E) Schematic.

manipulated with a 1064 nm trapping laser. When a laser trap was moved into close proximity to a mobile dandelion structure, the latter was pulled into the trap and held in a stable state in three dimensions. By bringing an optically trapped hybrid dandelion structure in solution into contact with the glass substrate, the material became quickly immobilized and resistant to further movement. Here, we believe the van der Waals force between the high surface area micelle arms, and hydrogen bonding between the Si–OH groups on the glass surface and the P2VP coronal segment are important. Because of the ease with which the hybrid structures trap, multiple dandelions could be deposited simultaneously or in quick succession.

With the control allowed by optical tweezers, the fabrication of arrays of completely customizable shape is possible. To demonstrate this we fabricated arrays of a variety of arrangements, from a smiley face to the letters UOB (Figure 4A–D).

Automation. To further enhance the efficiency of this process and remove the need for user direction, we created a program to automate the deposition process. This program is able to quickly detect, capture, and deposit multiple hybrid dandelion structures simultaneously, as shown schematically in Figure 5.

First, the user initializes the process by manually translating the stage to the desired initial deposition point. The program then proceeds to analyze the brightfield camera image and identify any hybrid dandelion structures within this region (Figure 5A). This is achieved using the LabVIEW vision acquisition toolbox, which searches the image for a predesignated shape. If no particles are identified within the field of view, the program instructs the motorized stage to move an incremental distance along the optical axis, so that an additional volume/area of the sample can be searched. When a hybrid structure is detected, the spatial light modulator is automatically reconfigured to place an optical trap at the location of the object (Figure 5B). Similarly, if multiple dandelions are detected, multiple optical traps are created. With multiple hybrid structures trapped, the positions of the optical traps are automatically reconfigured, moving the trapped objects into the configuration necessary to create the array design specified initially by the user (Figure 5C). To ensure that the object remains in a stable trapped state throughout the process, a maximum trap movement speed can be set by the user.

When automatically manipulating the positions of multiple objects simultaneously, it is necessary to ensure that collisions between trapped objects are prevented to stop any of the objects being knocked from their trap. Here we use an algorithm adapted from that reported by Chapin et al.[60] The program preemptively simulates each movement of the trapped hybrid structure to check for possible collisions. If an overlap is found, the planned movement is adjusted to prevent one object being knocked from its trap by another. To ensure that the micellar arms of the hybrid structures were kept separate, a safe minimum distance between two objects was initially set according to TEM images of the materials.

Having trapped and manipulated several hybrid structures in solution, the objects are automatically deposited on the surface by moving the focal plane to that initially specified as the substrate by the user. Using this method, large arrays can be quickly and automatically fabricated with reasonable accuracy. A 50 by 50 μm array comprising 100 objects (Supporting

DOI: 10.1021/acsnano.9b00342
ACS Nano XXXX, XXX, XXX–XXX

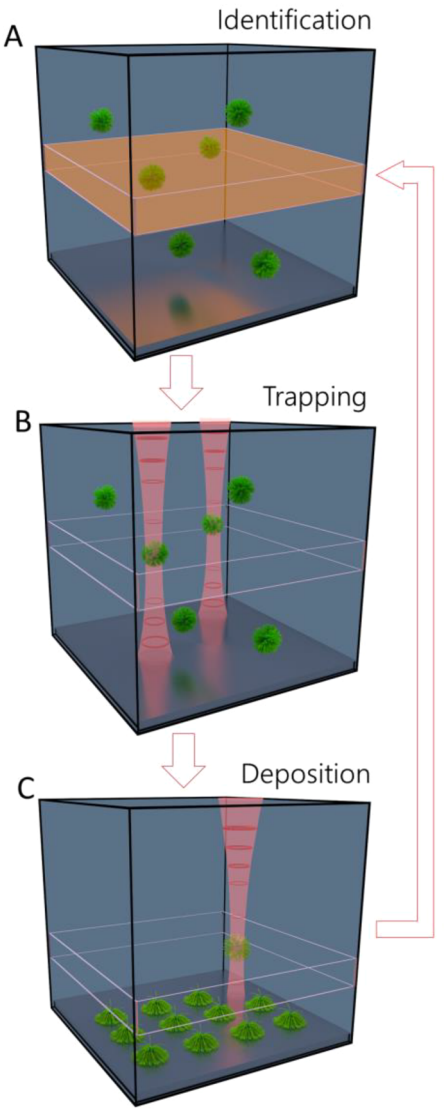

Figure 5. (A–C) Schematic showing the automated deposition process. (A) Identification. The current focal plane is scanned for objects matching the preprogrammed image of the hybrid structure. If no matching objects are found within the current focal plane, the *z* stage is moved to check another region. (B) Trapping. The SLM is reconfigured to place optical traps at the positions of the identified objects. (C) Deposition. The positons of the optical traps are moved in conjunction with the *z* position of the stage to deposit the trapped hybrids at the preprogrammed positions.

Information Figure 1) was fabricated in 10 min; with further optimization of the setup and materials we expect this process could be made substantially quicker and more precise. While this is still a long way from the rates needed for many industrial applications, it is an important step toward the production of smaller devices, sensors, and prototypes from block copolymer nanostructures.

CONCLUSIONS

In summary, we have demonstrated that through the combination of TIRF imaging and optical trapping we can precisely control the three-dimensional motion of individual cylindrical block copolymer micelles in solution. By directing the deposition of trapped single micelles, we were able to fabricate arrays with almost complete positional control. We also demonstrate how by utilizing dynamic holographic assembly the creation of ordered customizable arrays of complex hybrid block copolymer structures is possible. Such structures would be impossible to make using top-down or bottom-up methods alone. By automating the process using image matching and a collision avoidance algorithm, arrays containing hundreds of objects can be fabricated quickly and efficiently. The techniques described here should be applicable to a wide range of block copolymers with crystalline core-forming segments, including those with electroactivity,[38,46,47,61] enabling greater levels of solution-phase control and potentially facilitating the creation of micelle devices with a wide variety of potential applications.

METHODS

General Procedures and Materials. All polymerizations were carried out in an inert atmosphere glovebox. PFS_{56}-*b*-($PDMS_{775}$-r-$GreenDye_{20}$) (PDI = 1.23, the subscripts refer to the number-average degree of polymerization) was synthesized via living anionic ring-opening polymerization (ROP),[8] followed by postpolymerization derivitization.[62] The 900 nm silica beads were purchased from Bangs Laboratories. PFS_{63}-*b*-$PDMS_{513}$ and PFS_{20}-*b*-$P2VP_{140}$ were prepared by previously described methods involving living anionic ROP.[10,48]

Transmission Electron Microscopy (TEM). Samples for TEM were prepared by drop-casting 5 μL of the micelle solution onto a carbon coated copper grid which was placed on a piece of filter paper to remove excess solvent. Brightfield TEM micrographs were obtained on a JEOL1200EX II microscope operating at 120 kV and equipped with an SIS MegaViewIII digital camera.

Sample Preparation for Optical Tweezing with TIRF Apparatus. To produce a sample for the trapping experiments, a 50 mm borosilicate capillary tube (wall thickness 0.1 mm) was filled with a solution containing the block copolymer micelles. This capillary tube was then placed on a glass microscope slide where a small amount of epoxy adhesive was used to seal it at either end and fix it in place. Occasionally the surface of the capillary tube was found to be curved, disrupting the TIRF microscopy. As a result, for some of the experiments a small amount of micelle solution (approximately 10 μL) had to be drop cast onto a glass slide where a coverslip was placed on top and sealed round the edges with nail varnish. This produced a sample chamber which had a much smaller volume but still contained micelle solution.

Sample Preparation for Automated Deposition. To produce a sample for the trapping experiments, a 50 mm borosilicate capillary tube (wall thickness 0.1 mm) was filled with a solution containing the hybrid block copolymer structures. This capillary tube was then placed on a glass microscope slide where a small amount of epoxy adhesive was used to seal it at either end and fix it in place.

Optical Setup for TIRF Apparatus. The microscope was fitted with two stacked filter turrets. A Nikon TI-TIRF adapter was used to align a 488 nm laser beam (Omicron LightHUB) for TIRF and variable angle illumination. The dichroic elements and filter sets were optimized for 488 nm excitation and greater than 505 nm emission. This excitation wavelength was chosen to match the absorption spectra of the BODIPY FL dye attached to the corona of the micelles.

Images were recorded with an electron-multiplier charge-coupled device (Andor iXon EMCCD). The optical trap was created by coupling a 1090 nm laser (SPI) to an Elliot scientific E3500 system modified such that the beam diameter slightly underfilled the objective aperture. The optical trapping path is via the upper filter stack with a dichroic element that transmits light below 800 nm and reflects the 1090 nm laser beam. As a reference the trapping force exerted on polystyrene beads (1 μm diameter) dispersed in water measured using an escape force technique was 0.15 pN/mW.

Preparation of Crystallite Seed Micelles in EtOAc. A sample of long PFS_{63}-*b*-$PDMS_{513}$ cylinders (>10 μm) was prepared by heating a 1 mg/mL solution in EtOAc for 1 h at 75 °C and then allowing the sample to cool to room temperature and stand for 7 days. PFS_{63}-*b*-$PDMS_{513}$ crystallite seeds were then prepared by sonication of 4 mL of this

DOI: 10.1021/acsnano.9b00342
ACS Nano XXXX, XXX, XXX–XXX

solution for 4 h at 0 °C using a 50 W sonication processor equipped with a titanium sonotrode at 50% power. A stock solution (0.1 mg/mL, used in subsequent experiments) was prepared by diluting 1 mL of seeds in 9 mL of EtOAc.

L_n = 34 nm; L_w = 39 nm; PDI = 1.15; σL_n = 0.38; N = 253.

Preparation of Green Fluorescent Micelles. To a 7 mL screw-cap vial was added 1.9 mL of EtOAc and 100 μL of a 0.1 mg/mL solution of EtOAc seeds. To this mixture 65 μL of PFS_{56}-*b*-$PDMS_{775}$/$GREEN_{20}$ stock unimer solution (10 mg/mL in THF) was added while shaking.

L_n = 1073 nm; L_w = 1105 nm; PDI = 1.03; σ/L_n = 0.17; N = 208.

Structure of Green Fluorescent BCP.

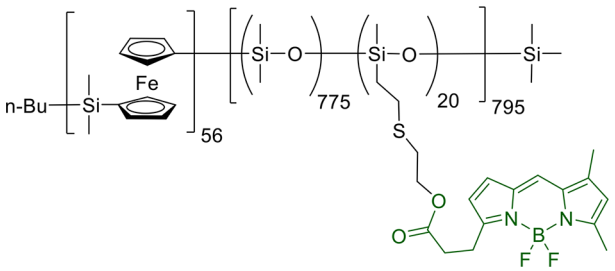

Polymer = PFS_{56}-*b*-($PDMS_{775}$/$GREEN_{20}$); M_n = 79,800; Block Ratio = 1:14; PDI = 1.23.

Preparation of Hybrid Block Copolymer Structures. A solution of 900 nm silica beads in isopropanol was added to a solution of stub-like PFS_{20}-*b*-$P2VP_{140}$ seed micelles in the same solvent (approximately 60 nm in length), such that hydrogen bonding causes the micelles to bond to the silica surface.

The excess seeds were then removed by centrifugation before additional PFS_{20}-*b*-$P2VP_{140}$ unimers in THF (20 μL of 10 mg/mL) were added to the seed coated beads in isopropanol (1 mL) causing the growth of extended cylindrical micelle arms from the exposed crystalline faces of the cylindrical micelle seeds attached to the central bead.

Automated Dynamic Holographic Assembly. One major obstacle which hindered the automated creation of large-scale micelle arrays was differentiating between a desirable single, unaggregated hybrid structure and the occasional aggregated larger structure, which when rotated along the *z* axis could appear identical. The other major hindrance was the uncontrolled sedimentation of the hybrid objects, causing them to become immobilized in undesirable locations. Both of these issues were overcome by using the top surface of the flow cell or capillary tube for the deposition process. This meant that no unwanted sedimentation could take place in the deposition area, and also that any large and therefore heavy aggregates dropped quickly out of the search area and remained unencountered. The automated deposition process was initiated by first setting the *z* position of the deposition surface. Next the deposition coordinates were loaded from a text document, and a previously taken brightfield optical microscope image of the desired object in the focal plane of the camera was loaded. Parameters such as the stage's speed of movement, *z* axis search interval, trap speed of movement, and the required match between the preset image of an object and the observed image could all be modified.

Optical Setup for Automated Deposition Experiments. Our system, similar to that described elsewhere,[58] is designed around a commercially available inverted microscope (Axiovert 200, Zeiss). A 3 W 1064 nm wavelength laser beam is expanded to fill an electrically addressed spatial light modulator (P512-0785, Boulder Nonlinear Systems) controlled using a LabVIEW (National Instruments) interface, with each hologram calculation performed on a PC graphics card (nVidia, Quadro FX 5600). The beam is then passed through a polarizing beam splitter and imaged onto the back aperture of an objective lens (1.3 NA 100× Plan-Neufluar, Zeiss). This simultaneously focuses the trapping beam creating the optical traps, and images the sample. Approximately 40% of the laser beam's power is passed by the objective and is shared between the traps. Movement of the field of view around the sample is achieved with a motorized x−y stage (MS2000, ASI) and a piezoelectric objective focusing system (Mipos 140 PL, Piezosystem Jena).

Custom Flow Cell Fabrication. To enable ease of use with a range of solvents, for the deposition experiments an adhesive-free fabrication process known as anodic bonding was used for the cell preparation of the cell.[63−65]

First, a rectangular channel was cut into a 1 mm thick piece of silicon wafer. Two holes, separated by the length of the channel, were then cut in a 1 mm thick piece of borosilicate glass chosen for its low coefficient of thermal expansion. This was then positioned on top of the silicon wafer, and both were placed in a box furnace. Graphite electrodes were positioned on top of and underneath the materials, before heating to 500 °C and applying a potential difference of 500 V across the materials. This caused the diffusion of dissociated oxygen ions in the glass to the boundary between the glass and silicon, forming silicon dioxide and generating a strong bond between the two layers.

PTFE tubes were then stretched and pulled through the holes until held snugly in place before being trimmed. A thin layer of parafilm was then stretched across the silicon wafer and a 0.1 mm thick coverslip clamped on top. The device was then heated to 60 °C sealing the coverslip in place, but allowing it to be removed after the deposition of BCP assemblies.

ASSOCIATED CONTENT

Supporting Information

The Supporting Information is available free of charge on the ACS Publications website at DOI: 10.1021/acsnano.9b00342.

Image showing an array of hybrid structures assembled using automated dynamic holographic assembly (PDF)

Video demonstrating the manipulation of a single block copolymer micelle in solution (AVI)

AUTHOR INFORMATION

Corresponding Authors

*(M.J.M.) E-mail: mervyn.miles@bristol.ac.uk.

*(I.M.) E-mail: imanners@uvic.ca.

ORCID

Oliver E. C. Gould: 0000-0002-8034-5724

Mitchell A. Winnik: 0000-0002-2673-2141

Ian Manners: 0000-0002-3794-967X

Present Address

#(O.E.C.G.) Institute of Biomaterial Science, Helmholtz-Zentrum Geesthacht, Teltow 14513, Germany.

Notes

The authors declare no competing financial interest.

ACKNOWLEDGMENTS

O.E.C.G. thanks the Bristol Center for Functional Nanomaterials (BCFN) Doctoral Training Center at Bristol funded by EPSRC, for a Ph.D. studentship. C.E.B. also thanks EPSRC for a Ph.D. studentship associated with the Center for Chemical Synthesis Doctoral Training Center at Bristol. S.J.B. thanks EPSRC for a Ph.D. studentship associated with the School of Physics at Bristol. I.M. thanks the EU for an ERC Advanced Investigator Grant. TEM studies were carried out in the Chemistry Imaging Facility at UoB with equipment funded by the UoB and EPSRC (EP/K035746/1).

REFERENCES

(1) Tritschler, U.; Pearce, S.; Gwyther, J.; Whittell, G. R.; Manners, I. 50th Anniversary Perspective: Functional Nanoparticles from the Solution Self-Assembly of Block Copolymers. *Macromolecules* **2017**, *50*, 3439−3463.

DOI: 10.1021/acsnano.9b00342
ACS Nano XXXX, XXX, XXX−XXX

(2) Jin, X.; Price, M. B.; Finnegan, J. R.; Boott, C. E.; Richter, J. M.; Rao, A.; Menke, S. M.; Friend, R. H.; Whittell, G. R.; Manners, I. Long-Range Exciton Transport in Conjugated Polymer Nanofibers Prepared by Seeded Growth. *Science* **2018**, *360*, 897−900.
(3) Elsabahy, M.; Wooley, K. L. Design of Polymeric Nanoparticles for Biomedical Delivery Applications. *Chem. Soc. Rev.* **2012**, *41*, 2545−2561.
(4) Schobel, J.; Burgard, M.; Hils, C.; Dersch, R.; Dulle, M.; Volk, K.; Karg, M.; Greiner, A.; Schmalz, H. Bottom-Up Meets Top-Down: Patchy Hybrid Nonwovens as an Efficient Catalysis Platform. *Angew. Chem., Int. Ed.* **2017**, *56*, 405−408.
(5) Mai, Y.; Eisenberg, A. Self-Assembly of Block Copolymers. *Chem. Soc. Rev.* **2012**, *41*, 5969−5985.
(6) Riess, G. Micellization of Block Copolymers. *Prog. Polym. Sci.* **2003**, *28*, 1107−1170.
(7) Gröschel, A. H.; Walther, A.; Löbling, T. I.; Schacher, F. H.; Schmalz, H.; Müller, A. H. E. Guided Hierarchical Co-Assembly of Soft Patchy Nanoparticles. *Nature* **2013**, *503*, 247−251.
(8) Hudson, Z. M.; Lunn, D. J.; Winnik, M. A.; Manners, I. Colour Tunable Fluorescent Multiblock Micelles. *Nat. Commun.* **2014**, *5*, 3372.
(9) O'Reilly, R. K.; Joralemon, M. J.; Wooley, K. L.; Hawker, C. J. Functionalization of Micelles and Shell Cross-Linked Nanoparticles Using Click Chemistry. *Chem. Mater.* **2005**, *17*, 5976−5988.
(10) Wang, H.; Patil, A. J.; Liu, K.; Petrov, S.; Mann, S.; Winnik, M. A.; Manners, I. Fabrication of Continuous and Segmented Polymer/Metal Oxide Nanowires Using Cylindrical Micelles and Block Comicelles as Templates. *Adv. Mater.* **2009**, *21*, 1805−1808.
(11) Bao, Y.; Wang, T.; Kang, Q.; Shi, C.; Ma, J. Micelle-Template Synthesis of Hollow Silica Spheres for Improving Water Vapor Permeability of Waterborne Polyurethane Membrane. *Sci. Rep.* **2017**, *7*, 46638.
(12) Freer, E. M.; Grachev, O.; Duan, X.; Martin, S.; Stumbo, D. P. High-Yield Self-Limiting Single-Nanowire Assembly with Dielectrophoresis. *Nat. Nanotechnol.* **2010**, *5*, 525−530.
(13) Raychaudhuri, S.; Dayeh, S. A.; Wang, D.; Yu, E. T. Precise Semiconductor Nanowire Placement through Dielectrophoresis. *Nano Lett.* **2009**, *9*, 2260−2266.
(14) Liu, M.; Lagdani, J.; Imrane, H.; Pettiford, C.; Lou, J.; Yoon, S.; Harris, V.; Vittoria, C.; Sun, N. X. Self-Assembled Magnetic Nanowire Arrays. *Appl. Phys. Lett.* **2007**, *90*, 103105.
(15) Tao, A.; Kim, F.; Hess, C.; Goldberger, J.; He, R. R.; Sun, Y. G.; Xia, Y. N.; Yang, P. D. Langmuir-Blodgett Silver Nanowire Monolayers for Molecular Sensing Using Surface-Enhanced Raman Spectroscopy. *Nano Lett.* **2003**, *3*, 1229−1233.
(16) Jin, S.; Whang, D.; McAlpine, M. C.; Friedman, R. S.; Wu, Y.; Lieber, C. M. Scalable Interconnection and Integration of Nanowire Devices Without Registration. *Nano Lett.* **2004**, *4*, 915−919.
(17) Huang, Y.; Lieber, C. M. Integrated Nanoscale Electronics and Optoelectronics: Exploring Nanoscale Science and Technology through Semiconductor Nanowires. *Pure Appl. Chem.* **2004**, *76*, 2051−2068.
(18) Huang, Y.; Duan, X.; Cui, Y.; Lauhon, L. J.; Kim, K. H.; Lieber, C. M. Logic Gates and Computation from Assembled Nanowire Building Blocks. *Science* **2001**, *294*, 1313−1317.
(19) Huang, Y.; Duan, X. F.; Wei, Q. Q.; Lieber, C. M. Directed Assembly of One-Dimensional Nanostructures into Functional Networks. *Science* **2001**, *291*, 630−633.
(20) Yao, J.; Yan, H.; Lieber, C. M. A Nanoscale Combing Technique for the Large-Scale Assembly of Highly Aligned Nanowires. *Nat. Nanotechnol.* **2013**, *8*, 329−335.
(21) Whang, D.; Jin, S.; Wu, Y.; Lieber, C. M. Large-Scale Hierarchical Organization of Nanowire Arrays for Integrated Nanosystems. *Nano Lett.* **2003**, *3*, 1255−1259.
(22) Ashkin, A. Acceleration and Trapping of Particles by Radiation Pressure. *Phys. Rev. Lett.* **1970**, *24*, 156.
(23) Kim, J. D.; Lee, Y. G. Construction and Actuation of a Microscopic Gear Assembly Formed Using Optical Tweezers. *J. Micromech. Microeng.* **2013**, *23*, 065010.
(24) Maragò, O. M.; Jones, P. H.; Gucciardi, P. G.; Volpe, G.; Ferrari, A. C. Optical Trapping and Manipulation of Nanostructures. *Nat. Nanotechnol.* **2013**, *8*, 807−819.
(25) Bergman, J.; Osunbayo, O.; Vershinin, M. Constructing 3D Microtubule Networks Using Holographic Optical Trapping. *Sci. Rep.* **2016**, *5*, 18085.
(26) Wang, X.; Chen, S.; Kong, M.; Wang, Z.; Costa, K. D.; Li, R. A.; Sun, D. Enhanced Cell Sorting and Manipulation with Combined Optical Tweezer and Microfluidic Chip Technologies. *Lab Chip* **2011**, *11*, 3656.
(27) Rouger, V.; Bordet, G.; Couillault, C.; Monneret, S.; Mailfert, S.; Ewbank, J. J.; Pujol, N.; Marguet, D. Independent Synchronized Control and Visualization of Interactions Between Living Cells and Organisms. *Biophys. J.* **2014**, *106*, 2096−2104.
(28) Zhang, H.; Liu, K. K. Optical Tweezers for Single Cells. *J. R. Soc., Interface* **2008**, *5*, 671−690.
(29) Melzer, J. E.; McLeod, E. Fundamental Limits of Optical Tweezer Nanoparticle Manipulation Speeds. *ACS Nano* **2018**, *12*, 2440−2447.
(30) Gensch, T.; Hofkens, J.; van Stam, J.; Faes, H.; Creutz, S.; Tsuda, K.; Jérôme, R.; Masuhara, H.; De Schryver, F. C. Transmission and Confocal Fluorescence Microscopy and Time-Resolved Fluorescence Spectroscopy Combined with a Laser Trap: Investigation of Optically Trapped Block Copolymer Micelles. *J. Phys. Chem. B* **1998**, *102*, 8440−8451.
(31) Ito, S.; Yoshikawa, H.; Masuhara, H. Optical Patterning and Photochemical Fixation of Polymer Nanoparticles on Glass Substrates. *Appl. Phys. Lett.* **2001**, *78*, 2566−2568.
(32) Hotta, J.; Sasaki, K.; Masuhara, H.; Morishima, Y. Laser-Controlled Assembling of Repulsive Unimolecular Micelles in Aqueous Solution. *J. Phys. Chem. B* **1998**, *102*, 7687.
(33) Gould, O. E. C.; Qiu, H.; Lunn, D. J.; Rowden, J.; Harniman, R. L.; Hudson, Z. M.; Winnik, M. A.; Miles, M. J.; Manners, I. Transformation and Patterning of Supermicelles Using Dynamic Holographic Assembly. *Nat. Commun.* **2015**, *6*, 10009.
(34) Schmelz, J.; Schedl, A. E.; Steinlein, C.; Manners, I.; Schmalz, H. Length Control and Block-Type Architectures in Worm-like Micelles with Polyethylene Cores. *J. Am. Chem. Soc.* **2012**, *134*, 14217−14225.
(35) Schmelz, J.; Karg, M.; Hellweg, T.; Schmalz, H. General Pathway toward Crystalline-Core Micelles with Tunable Morphology and Corona Segregation. *ACS Nano* **2011**, *5*, 9523−9534.
(36) Qian, J.; Li, X.; Lunn, D. J.; Gwyther, J.; Hudson, Z. M.; Kynaston, E.; Rupar, P. A.; Winnik, M. A.; Manners, I. Uniform, High Aspect Ratio Fiber-like Micelles and Block Co-Micelles with a Crystalline π-Conjugated Polythiophene Core by Self-Seeding. *J. Am. Chem. Soc.* **2014**, *136*, 4121−4124.
(37) Lee, E.; Hammer, B.; Kim, J. K.; Page, Z.; Emrick, T.; Hayward, R. C. Hierarchical Helical Assembly of Conjugated Poly(3-Hexylthiophene)-Block- Poly(3-Triethylene Glycol Thiophene) Diblock Copolymers. *J. Am. Chem. Soc.* **2011**, *133*, 10390−10393.
(38) Park, S. J.; Kang, S. G.; Fryd, M.; Saven, J. G.; Park, S. J. Highly Tunable Photoluminescent Properties of Amphiphilic Conjugated Block Copolymers. *J. Am. Chem. Soc.* **2010**, *132*, 9931−9933.
(39) Gao, Y.; Li, X.; Hong, L.; Liu, G. Mesogen-Driven Formation of Triblock Copolymer Cylindrical Micelles. *Macromolecules* **2012**, *45*, 1321−1330.
(40) Mihut, A. M.; Drechsler, M.; Möller, M.; Ballauff, M. Sphere-to-Rod Transition of Micelles Formed by the Semicrystalline Polybutadiene-Block-Poly(Ethylene Oxide) Block Copolymer in a Selective Solvent. *Macromol. Rapid Commun.* **2010**, *31*, 449−453.
(41) Du, Z. X.; Xu, J. T.; Fan, Z. Q. Micellar Morphologies of Poly(ε-Caprolactone)-*b*-Poly(Ethylene Oxide) Block Copolymers in Water with a Crystalline Core. *Macromolecules* **2007**, *40*, 7633−7637.
(42) Petzetakis, N.; Walker, D.; Dove, A. P.; O'Reilly, R. K. Crystallization-Driven Sphere-to-Rod Transition of Poly(Lactide)-b-Poly(Acrylic Acid) Diblock Copolymers: Mechanism and Kinetics. *Soft Matter* **2012**, *8*, 7408−7414.

DOI: 10.1021/acsnano.9b00342
ACS Nano XXXX, XXX, XXX−XXX

(43) Pitto-Barry, A.; Kirby, N.; Dove, A. P.; O'Reilly, R. K. Expanding the Scope of the Crystallization-Driven Self-Assembly of Polylactide-Containing Polymers. *Polym. Chem.* **2014**, *5*, 1427.
(44) Lazzari, M.; Scalarone, D.; Vazquez-Vazquez, C.; López-Quintela, M. A. Cylindrical Micelles from the Self-Assembly of Polyacrylonitrile-Based Diblock Copolymers in Nonpolar Selective Solvents. *Macromol. Rapid Commun.* **2008**, *29*, 352−357.
(45) Gädt, T.; Ieong, N. S.; Cambridge, G.; Winnik, M. A.; Manners, I. Complex and Hierarchical Micelle Architectures from Diblock Copolymers Using Living, Crystallization-Driven Polymerizations. *Nat. Mater.* **2009**, *8*, 144−150.
(46) Gwyther, J.; Gilroy, J. B.; Rupar, P. A.; Lunn, D. J.; Kynaston, E.; Patra, S. K.; Whittell, G. R.; Winnik, M. A.; Manners, I. Dimensional Control of Block Copolymer Nanofibers with a π-Conjugated Core: Crystallization-Driven Solution Self-Assembly of Amphiphilic Poly(3-Hexylthiophene)-*b*-Poly(2-Vinylpyridine). *Chem. - Eur. J.* **2013**, *19*, 9186−9197.
(47) Lee, I. H.; Amaladass, P.; Yoon, K. Y.; Shin, S.; Kim, Y. J.; Kim, I.; Lee, E.; Choi, T. L. Nanostar and Nanonetwork Crystals Fabricated by *in Situ* Nanoparticlization of Fully Conjugated Polythiophene Diblock Copolymers. *J. Am. Chem. Soc.* **2013**, *135*, 17695−17698.
(48) Hailes, R. L. N.; Oliver, A. M.; Gwyther, J.; Whittell, G. R.; Manners, I. Polyferrocenylsilanes: Synthesis, Properties, and Applications. *Chem. Soc. Rev.* **2016**, *45*, 5358−5407.
(49) Paquet, C.; Cyr, P. W.; Kumacheva, E.; Manners, I. Rationalized Approach to Molecular Tailoring of Polymetallocenes with Predictable Optical Properties. *Chem. Mater.* **2004**, *16*, 5205−5211.
(50) Gilroy, J. B.; Rupar, P. A.; Whittell, G. R.; Chabanne, L.; Terrill, N. J.; Winnik, M. A.; Manners, I.; Richardson, R. M. Probing the Structure of the Crystalline Core of Field-Aligned, Monodisperse, Cylindrical Polyisoprene-Block-Polyferrocenylsilane Micelles in Solution Using Synchrotron Small- and Wide-Angle X-Ray Scattering. *J. Am. Chem. Soc.* **2011**, *133*, 17056−17062.
(51) Ku, K. H.; Kim, M. P.; Paek, K.; Shin, J. M.; Chung, S.; Jang, S. G.; Chae, W.-S.; Yi, G. R.; Kim, B. J. Multicolor Emission of Hybrid Block Copolymer-Quantum Dot Microspheres by Controlled Spatial Isolation of Quantum Dots. *Small* **2013**, *9*, 2667−2672.
(52) Shrestha, R.; Elsabahy, M.; Luehmann, H.; Samarajeewa, S.; Florez-Malaver, S.; Lee, N. S.; Welch, M. J.; Liu, Y.; Wooley, K. L. Hierarchically Assembled Theranostic Nanostructures for SiRNA Delivery and Imaging Applications. *J. Am. Chem. Soc.* **2012**, *134*, 17362−17365.
(53) Yan, X.; Liu, G.; Liu, F.; Tang, B.; Peng, H.; Pakhomov, A. B.; Wong, C. Y. Superparamagnetic Triblock Copolymer/Fe_2O_3 Hybrid Nanofibers. *Angew. Chem., Int. Ed.* **2001**, *40*, 3593−3596.
(54) Li, X.; Wolanin, P. J.; MacFarlane, L. R.; Harniman, R. L.; Qian, J.; Gould, O. E. C.; Dane, T. G.; Rudin, J.; Cryan, M. J.; Schmaltz, T.; Frauenrath, H.; Winnik, M. A.; Faul, C. F. J.; Manners, I. Uniform Electroactive Fibre-like Micelle Nanowires for Organic Electronics. *Nat. Commun.* **2017**, *8*, 15909.
(55) Cativo, M. H. M.; Kim, D. K.; Riggleman, R. A.; Yager, K. G.; Nonnenmann, S. S.; Chao, H.; Bonnell, D. A.; Black, C. T.; Kagan, C. R.; Park, S. J. Air-Liquid Interfacial Self-Assembly of Conjugated Block Copolymers into Ordered Nanowire Arrays. *ACS Nano* **2014**, *8*, 12755−12762.
(56) Müllner, M.; Yuan, J.; Weiss, S.; Walther, A.; Förtsch, M.; Drechsler, M.; Müller, A. H. E. Water-Soluble Organo-Silica Hybrid Nanotubes Templated by Cylindrical Polymer Brushes. *J. Am. Chem. Soc.* **2010**, *132*, 16587−16592.
(57) Pauzauskie, P. J.; Radenovic, A.; Trepagnier, E.; Shroff, H.; Yang, P.; Liphardt, J. Optical Trapping and Integration of Semiconductor Nanowire Assemblies in Water. *Nat. Mater.* **2006**, *5*, 97−101.
(58) Gibson, G.; Carberry, D.; Whyte, G.; Leach, J.; Courtial, J.; Jackson, J.; Robert, D.; Miles, M.; Padgett, M. Holographic Assembly Workstation for Optical Manipulation. *J. Opt. A: Pure Appl. Opt.* **2008**, *10*, 044009.
(59) Jia, L.; Zhao, G.; Shi, W.; Coombs, N.; Gourevich, I.; Walker, G. C.; Guerin, G.; Manners, I.; Winnik, M. A. A Design Strategy for the Hierarchical Fabrication of Colloidal Hybrid Mesostructures. *Nat. Commun.* **2014**, *5*, 3882.
(60) Chapin, S. C.; Germain, V.; Dufresne, E. R. Automated Trapping, Assembly, and Sorting with Holographic Optical Tweezers. *Opt. Express* **2006**, *14*, 13095−13100.
(61) Kim, Y.; Cho, C.; Paek, K.; Jo, M.; Park, M.; Lee, N.; Kim, Y.; Kim, B. J.; Lee, E. Precise Control of Quantum Dot Location within the P3HT- *b* - P2VP/QD Nanowires Formed by Crystallization-Driven 1D Growth of Hybrid Dimeric Seeds. *J. Am. Chem. Soc.* **2014**, *136*, 2767.
(62) Hudson, Z. M.; Boott, C. E.; Robinson, M. E.; Rupar, P. A.; Winnik, M. A.; Manners, I. Tailored Hierarchical Micelle Architectures Using Living Crystallization-Driven Self-Assembly in Two Dimensions. *Nat. Chem.* **2014**, *6*, 893−898.
(63) Wallis, G.; Pomerantz, D. I. Field Assisted Glass-Metal Sealing. *J. Appl. Phys.* **1969**, *40*, 3946.
(64) Leib, J.; Hansen, U.; Maus, S.; Feindt, H.; Hauck, K.; Zoschke, K.; Toepper, M. Anodic Bonding at Low Voltage Using Micro-structured Borosilicate Glass Thin-Films. *Electronics System Integration Technology Conference, ESTC 2010 - Proceedings*; IEEE: 2010.
(65) Gerlach, A.; Maas, D.; Seidel, D.; Bartuch, H.; Schundau, S.; Kaschlik, K. Low-Temperature Anodic Bonding of Silicon to Silicon Wafers by Means of Intermediate Glass Layers. *Microsyst. Technol.* **1999**, *5*, 144−149.

DOI: 10.1021/acsnano.9b00342
ACS Nano XXXX, XXX, XXX−XXX